This journal is © the Owner Societies 2010

Supporting Information for

Characterization of large vacancy clusters in diamond from a generational algorithm using tight binding density functional theory

Brad Slepetz, Istvan Laszlo,[a] Yury Gogotsi,[b] David Hyde-Volpe, and Miklos Kertesz[*]

Chemistry Department, Georgetown University, 37th and O Streets, NW, Washington, DC, 20057-1227

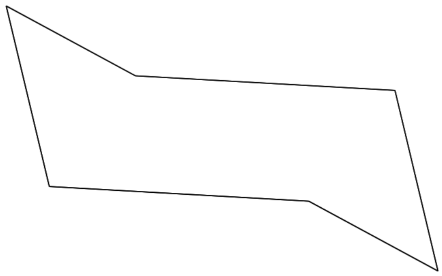

V_6

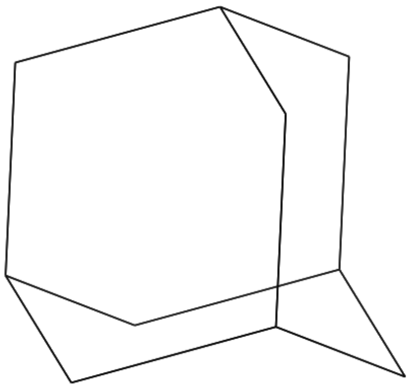

V_{10}

[a] Department of Theoretical Physics, Institute of Physics, Budapest University of Technology and Economics, Budapest, H-1521, Hungary.
[b] Department of Materials Science and Engineering, Drexel University, Philadelphia, PA, 19104, USA.
[*] Corresponding author. E-mail: Kertesz@georgetown.edu

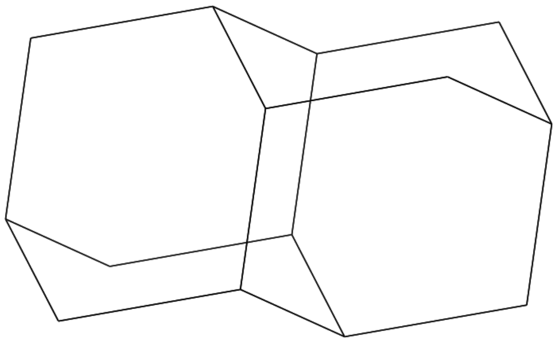

V_{14}

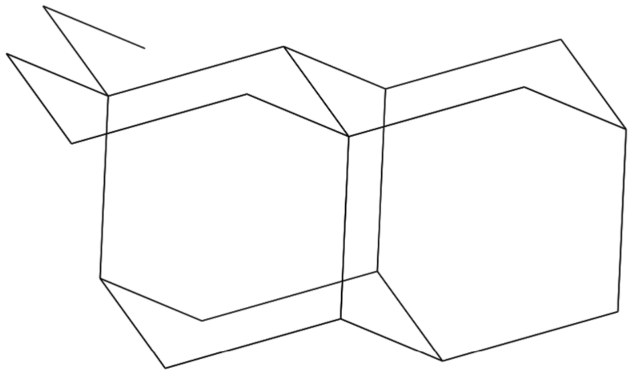

V_{19}

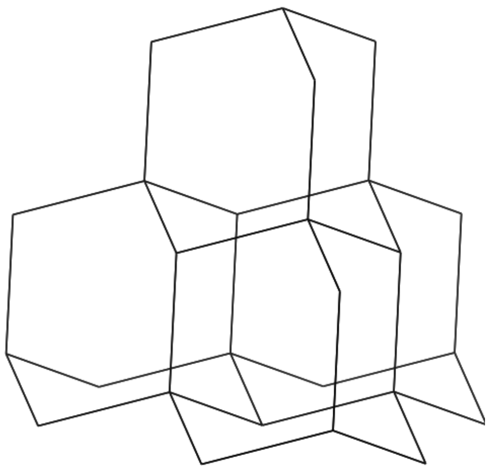

V_{26}

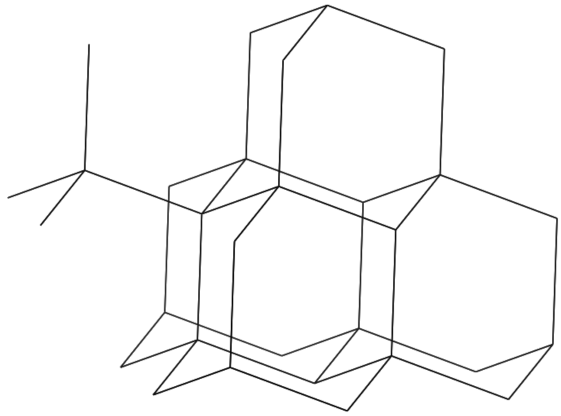

V_{30}

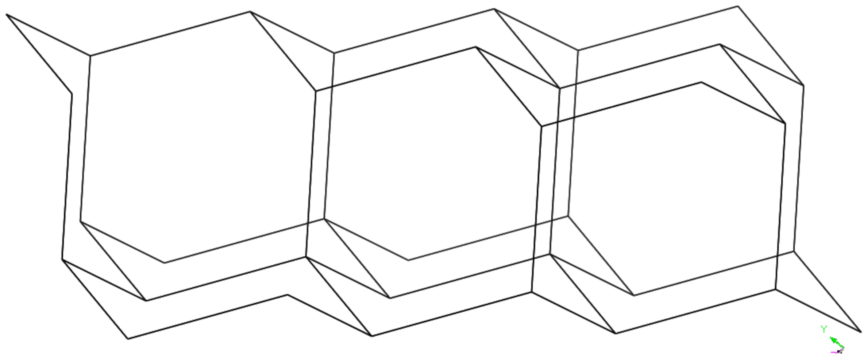

V_{35}

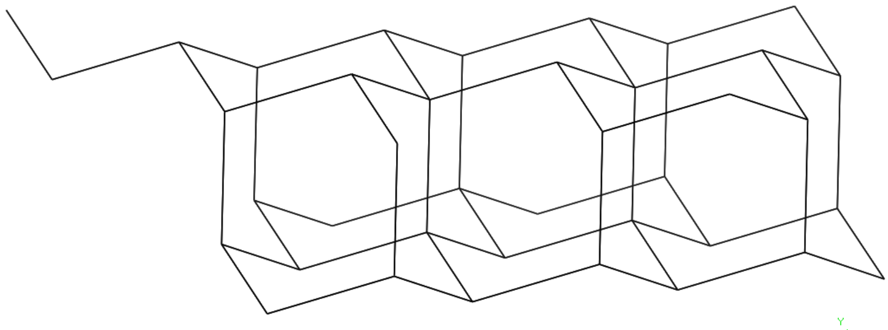

V_{39}

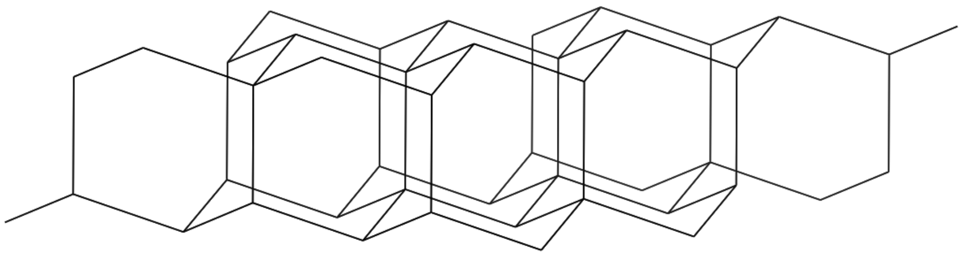

V_{45}

This journal is © the Owner Societies 2010

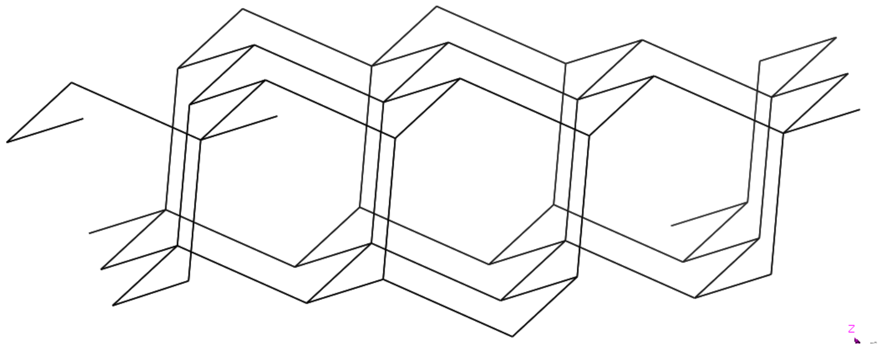

V_{50}

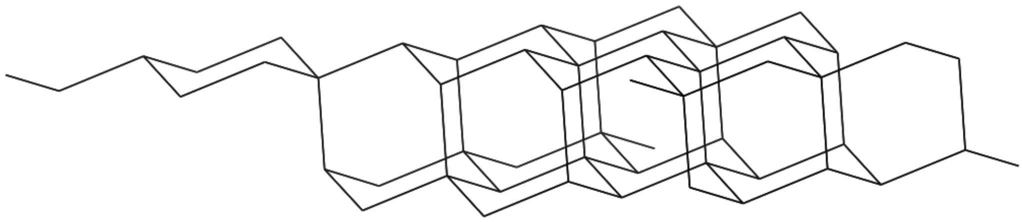

V_{54}

Figure S1. Unrelaxed structures of selected vacancy clusters V_n (n=6, 10, 14, 19, 26, 30, 35, 39, 45, 50, 54). Not that these structures turned out to be the most stable for the given n after geometry relaxation

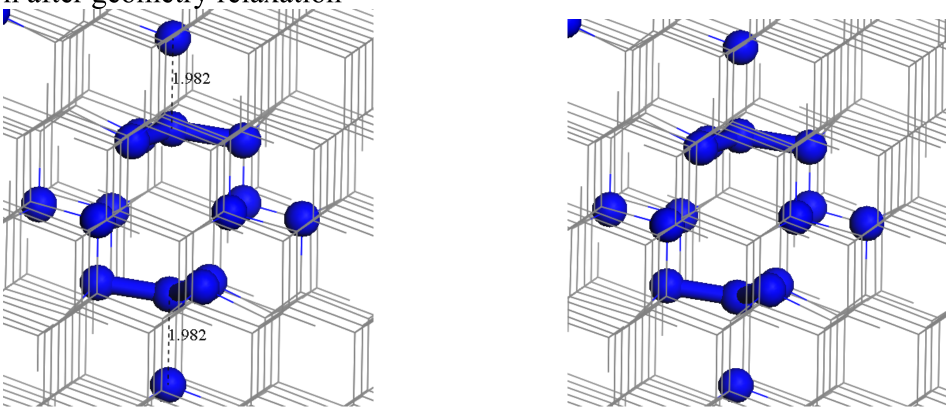

V_6

This journal is © the Owner Societies 2010

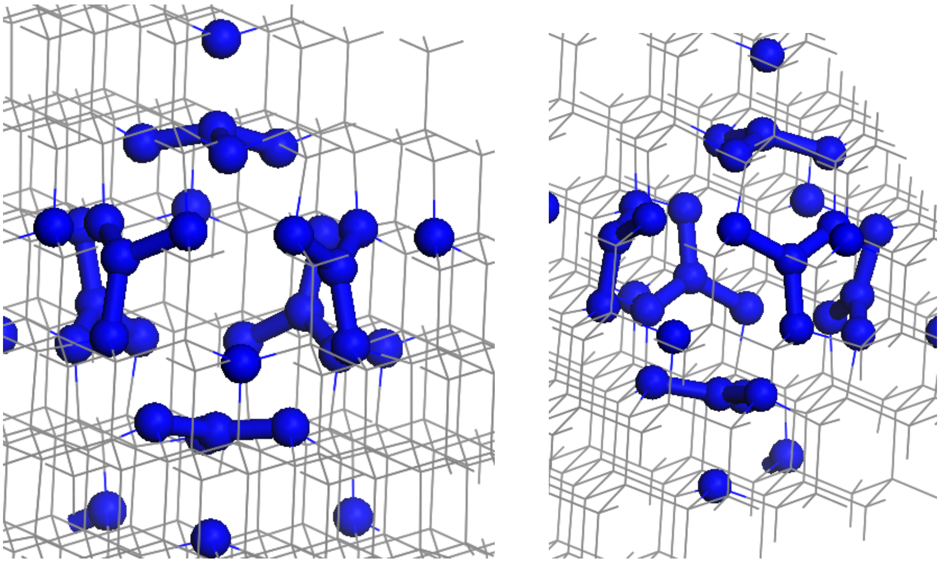

V_{14}

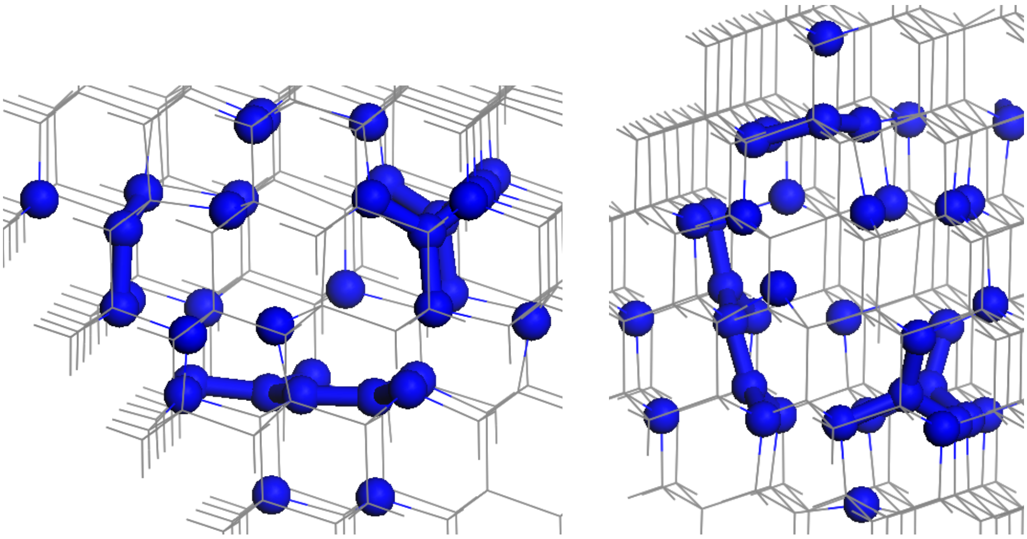

V_{19}

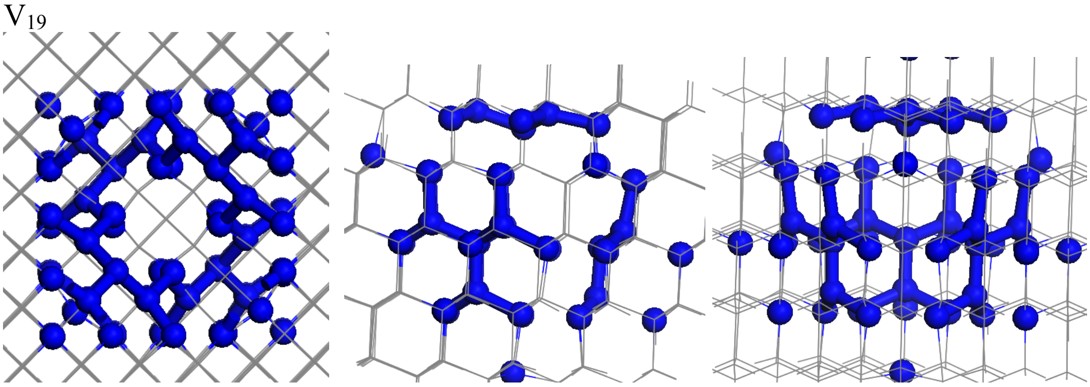

V_{26}

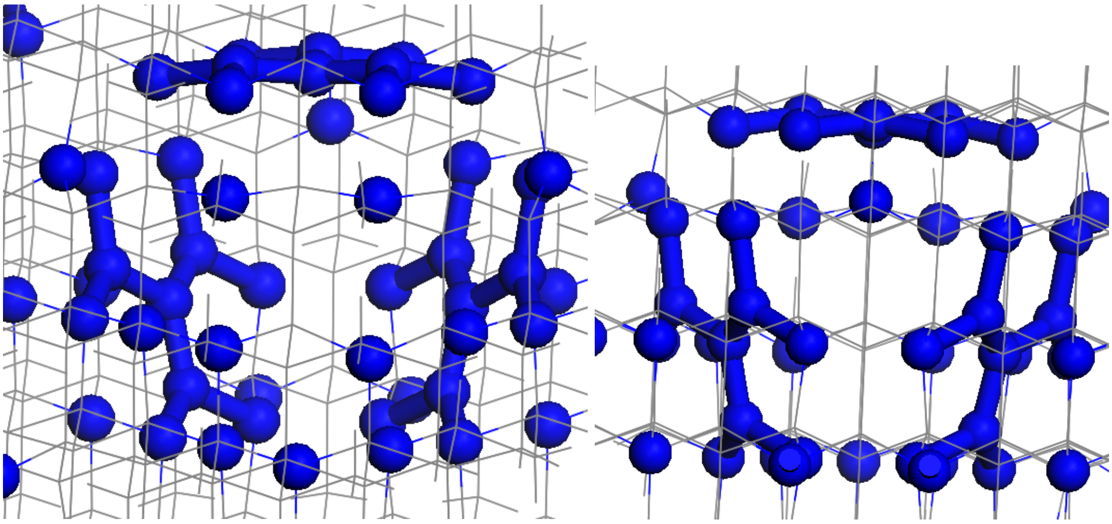

V_{30}

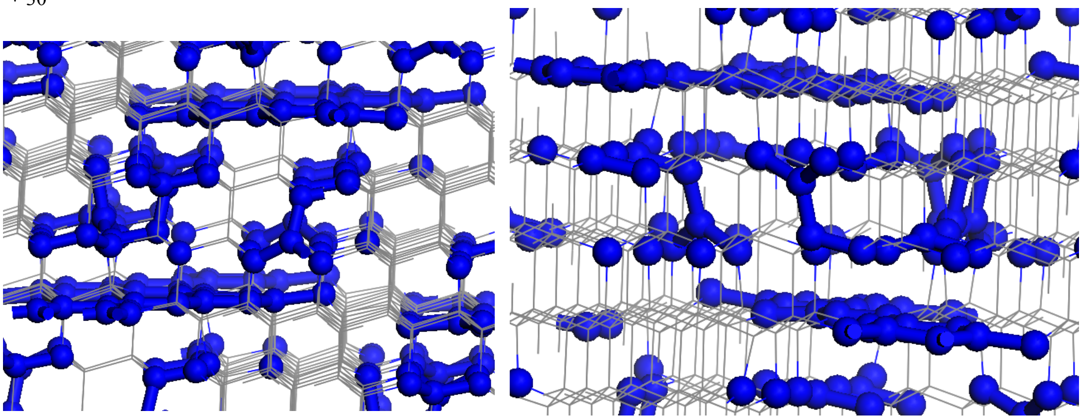

V_{39}

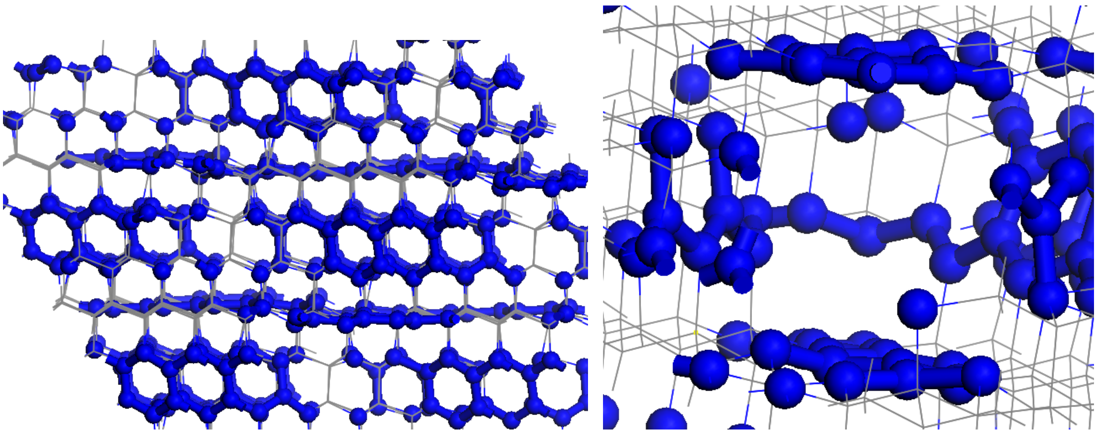

V_{45}

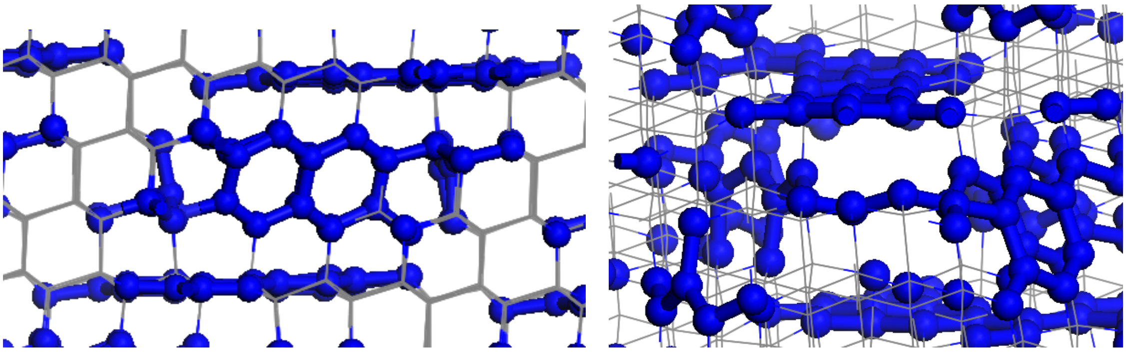

V_{50}

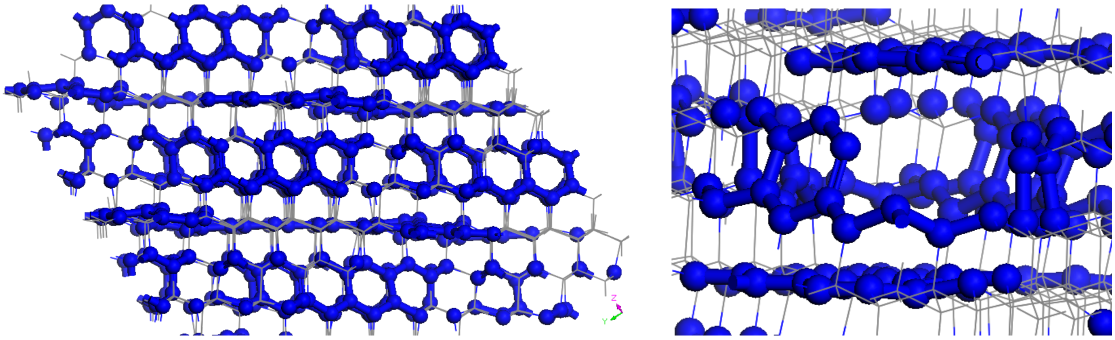

V_{54}

.

Figure S2. Relaxed structures of selected vacancy clusters V_n (n=6, 14, 19, 26, 30, 39, 45, 50, 54). These structures are the most stable for the given n values. Larger blue atoms indicate those that are adjacent to the pore left by the vacancy cluser and undergo the largest rearrangement upon relaxation. As n increases, regions of local graphitization become energetically favorable. For each V_n different views are provided to aid the visualization.

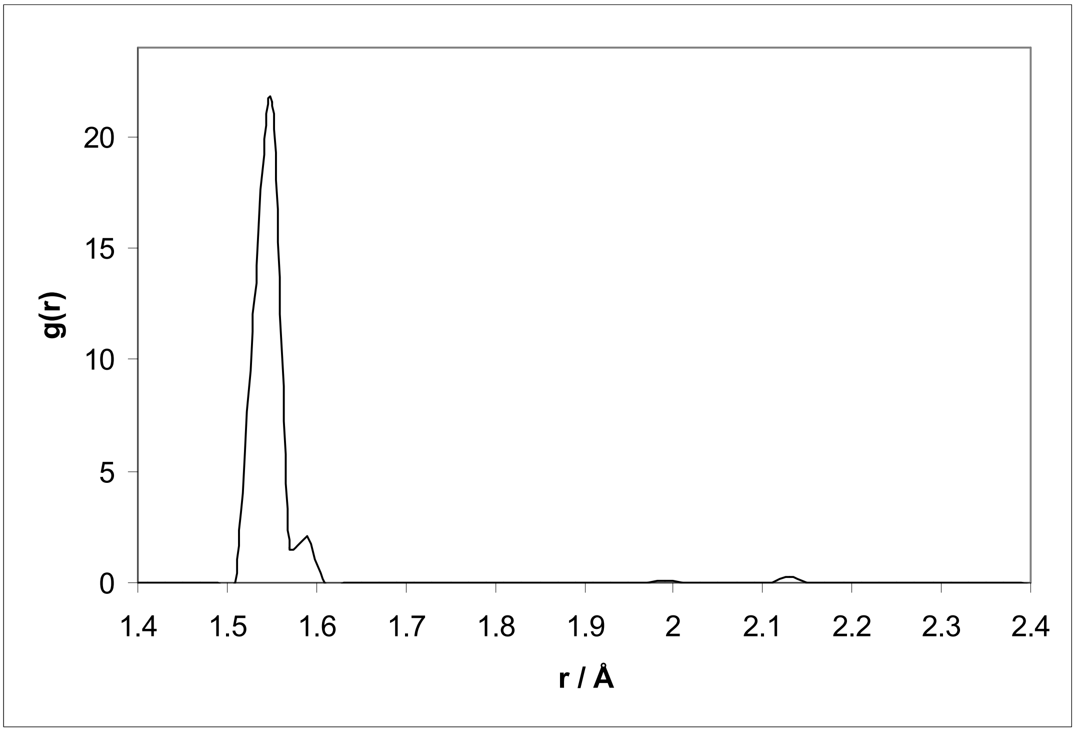
g(r)
0
5
10
15
20
1.4
1.5
1.6
1.7
1.8
1.9
2
2.1
2.2
2.3
2.4
r / Å

V_6

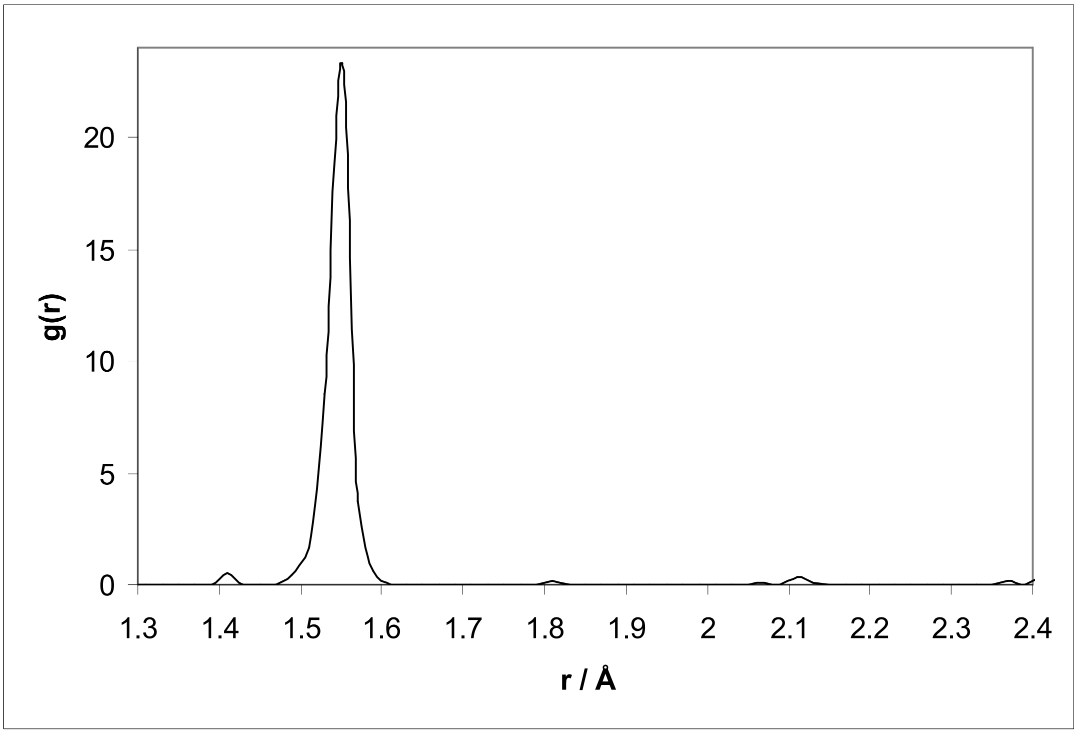
g(r)
0
5
10
15
20
1.3
1.4
1.5
1.6
1.7
1.8
1.9
2
2.1
2.2
2.3
2.4
r / Å

V_{14}

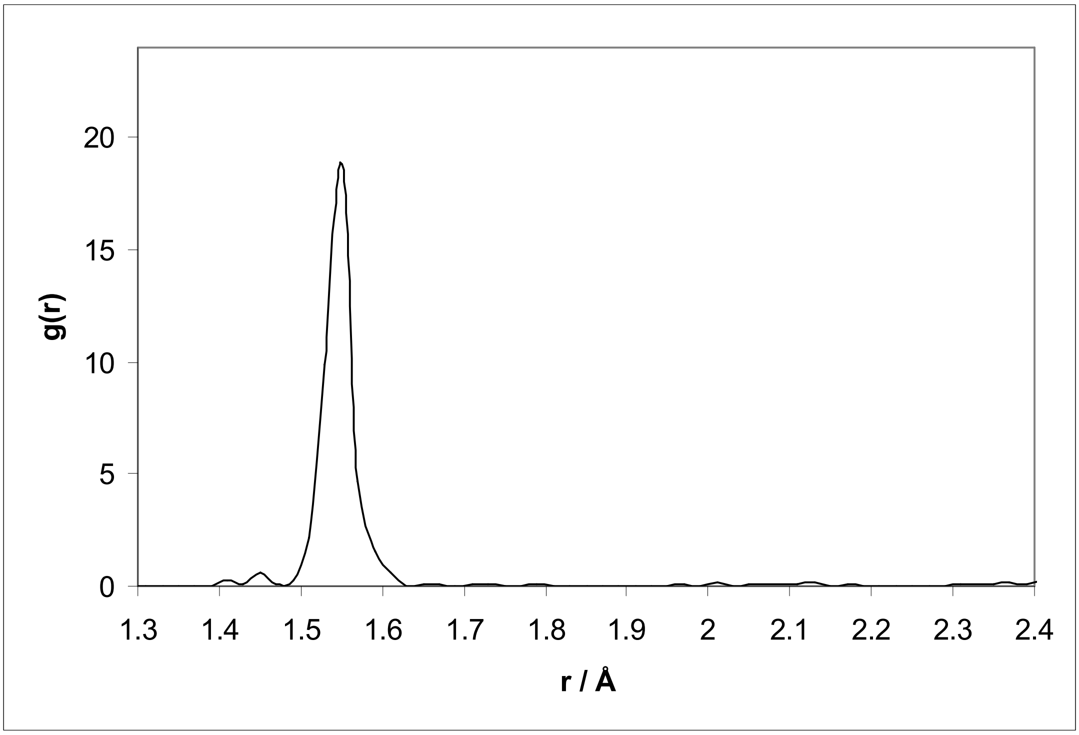
g(r)
0
5
10
15
20
1.3
1.4
1.5
1.6
1.7
1.8
1.9
2
2.1
2.2
2.3
2.4
r / Å

V_{19}

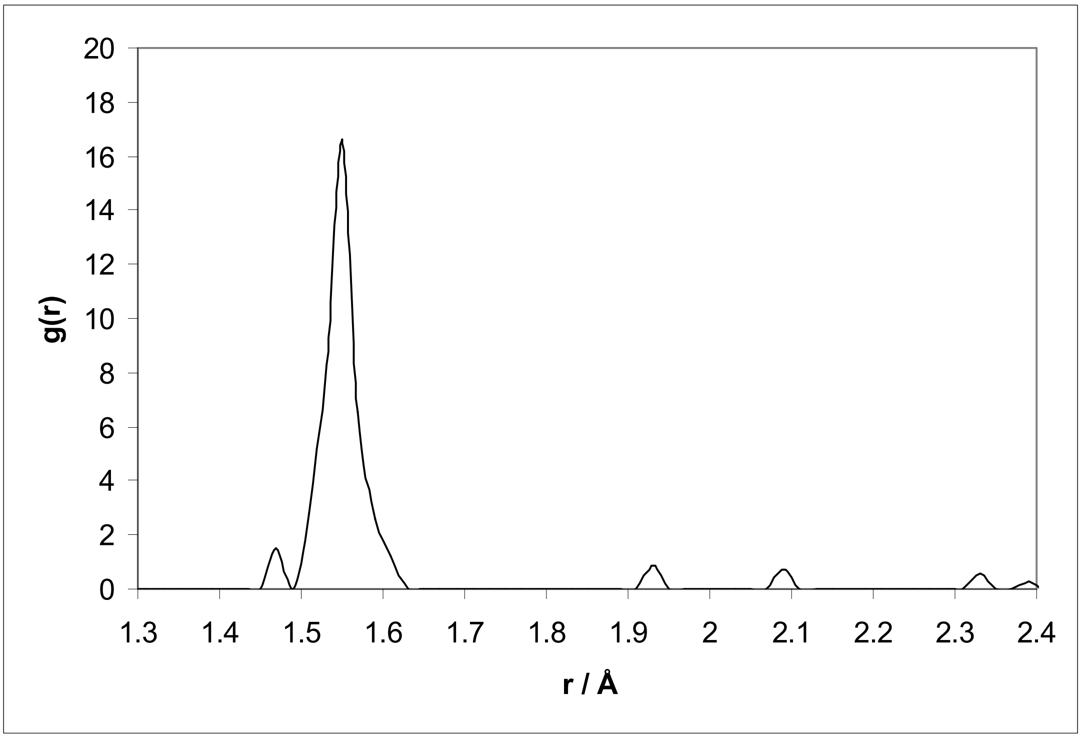
g(r)
0
2
4
6
8
10
12
14
16
18
20
1.3
1.4
1.5
1.6
1.7
1.8
1.9
2
2.1
2.2
2.3
2.4
r / Å

V_{26}

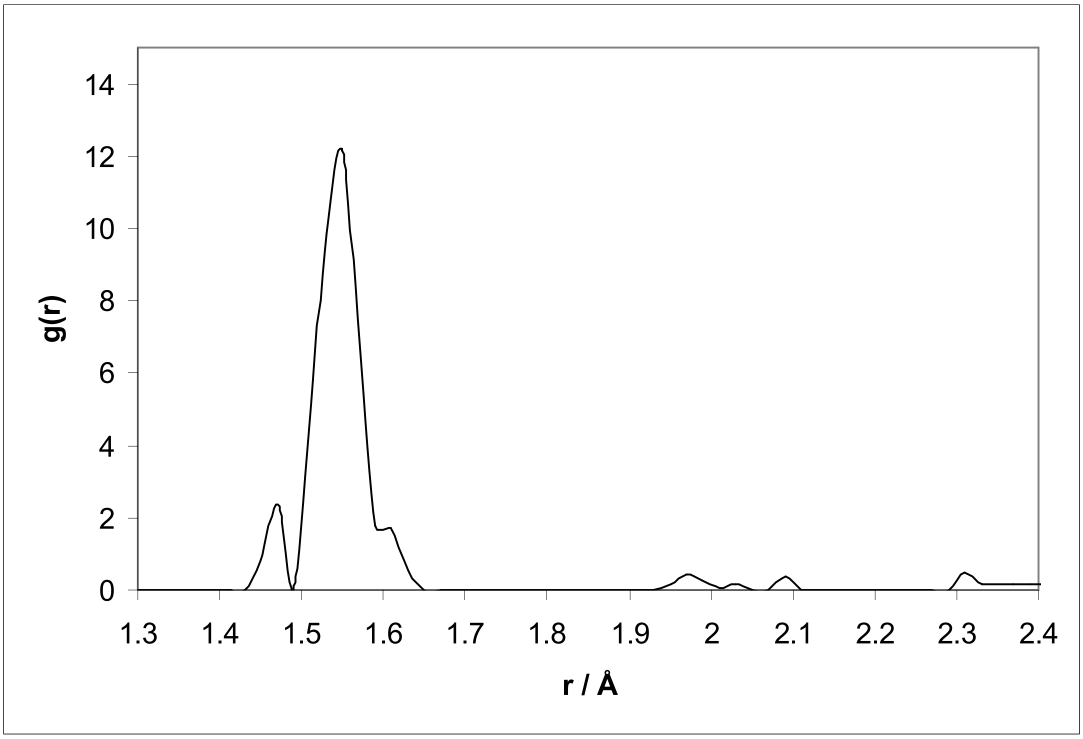
g(r)
0
2
4
6
8
10
12
14
1.3
1.4
1.5
1.6
1.7
1.8
1.9
2
2.1
2.2
2.3
2.4
r / Å

V_{30}

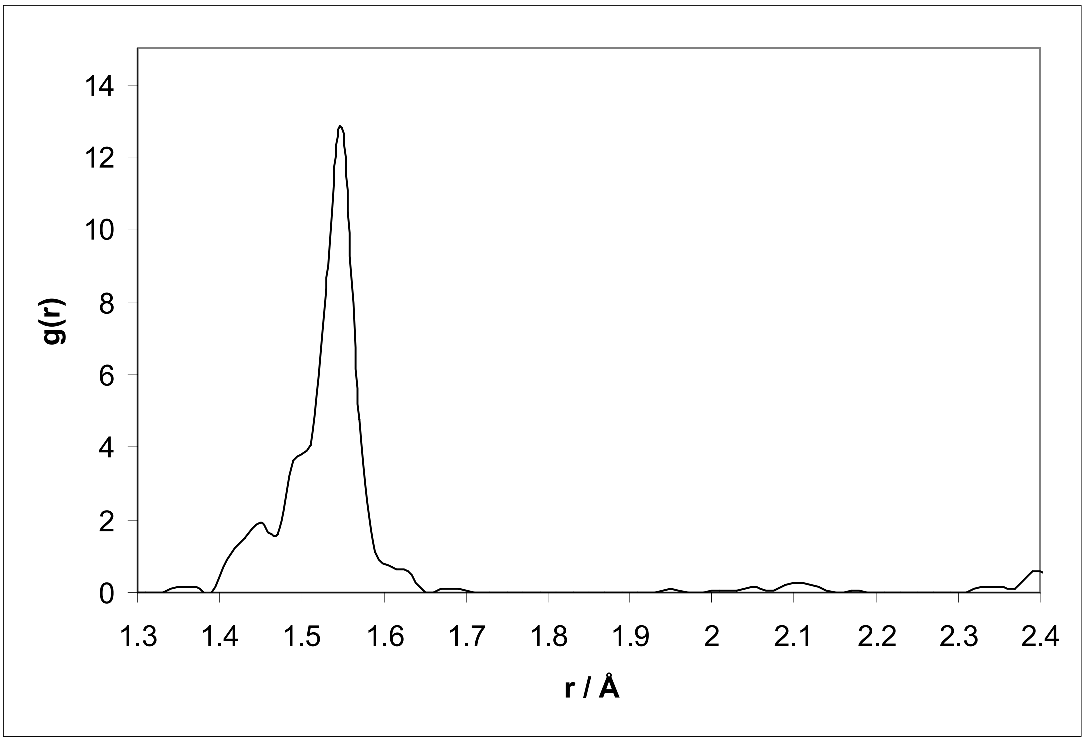
g(r)
0
2
4
6
8
10
12
14
1.3
1.4
1.5
1.6
1.7
1.8
1.9
2
2.1
2.2
2.3
2.4
r / Å

V_{39}

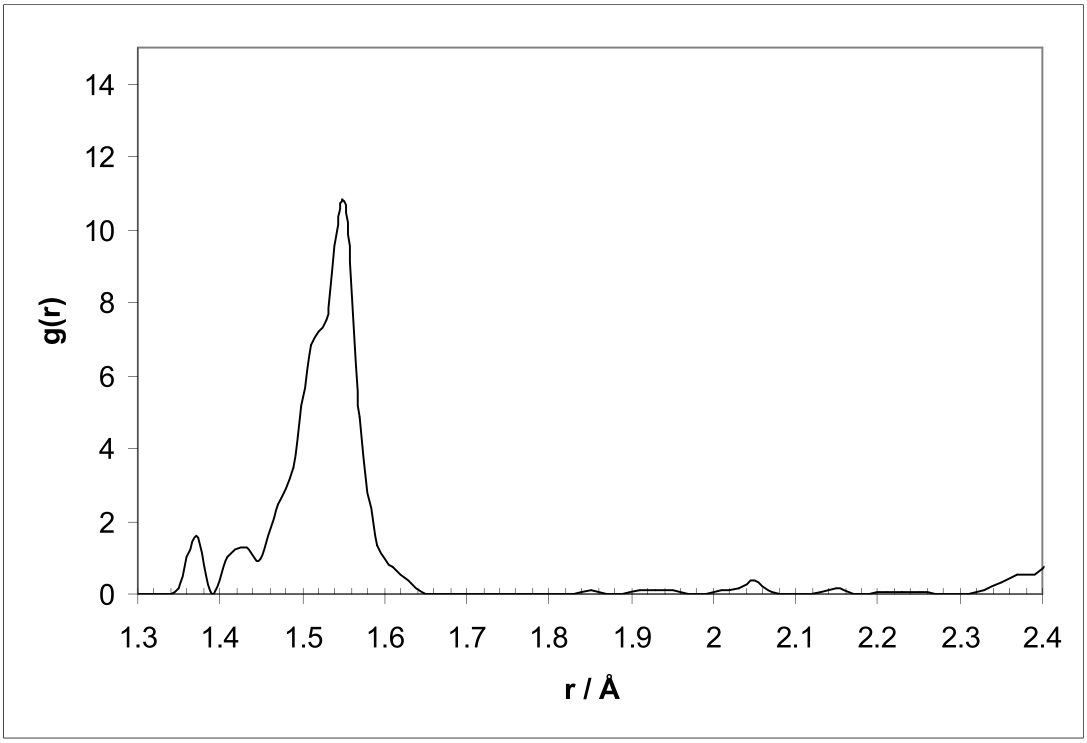
g(r)
14
12
10
8
6
4
2
0
1.3
1.4
1.5
1.6
1.7
1.8
1.9
2
2.1
2.2
2.3
2.4
r / Å

V_{45}

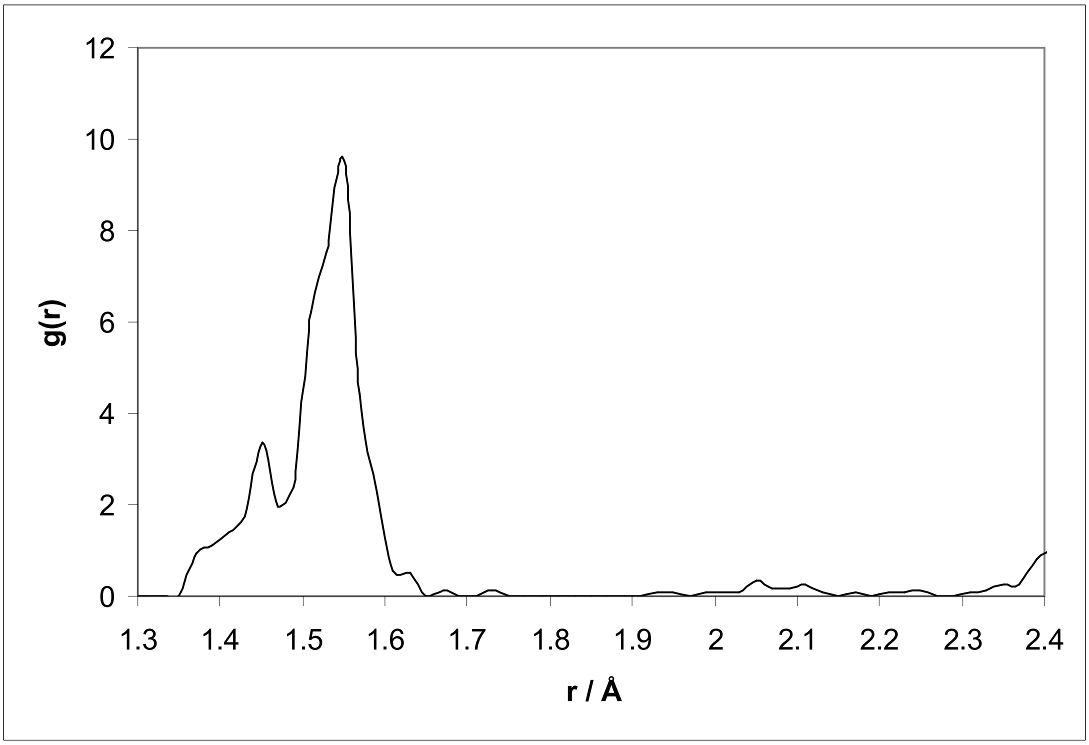
g(r)
12
10
8
6
4
2
0
1.3
1.4
1.5
1.6
1.7
1.8
1.9
2
2.1
2.2
2.3
2.4
r / Å

V_{50}

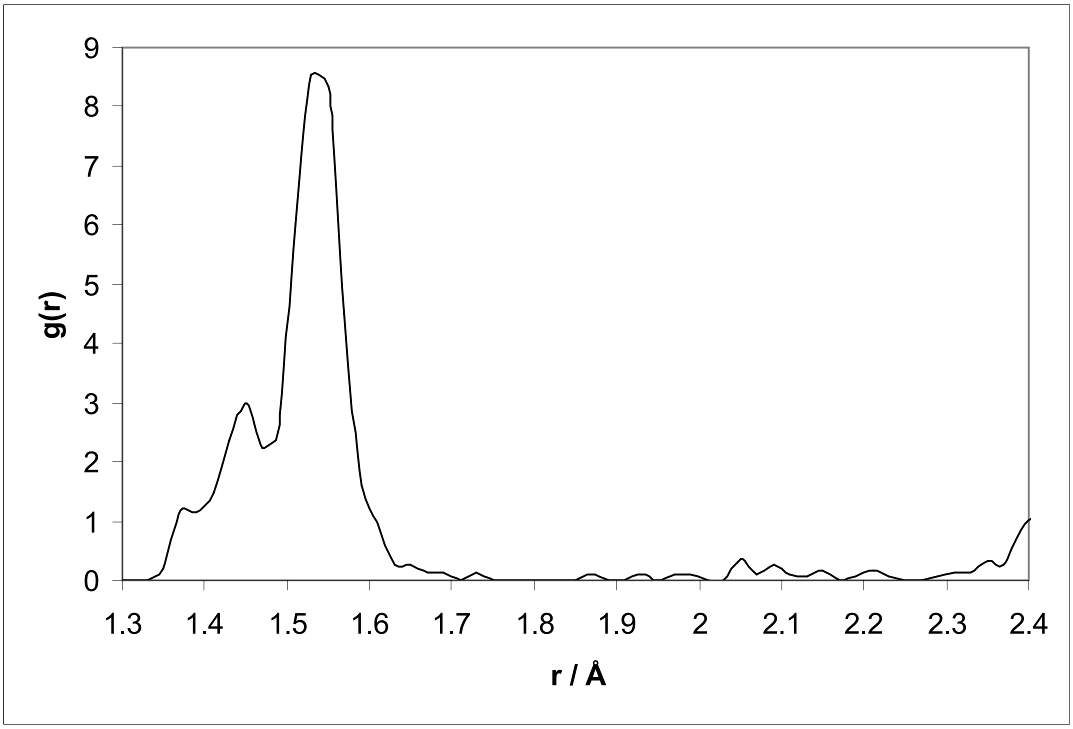

V_{54}

Figure S3. Calculated pair correlation function, g(*r*) for V_n in the 1.3 Å < *r* < 2.4 Å range. (n=6, 14, 19, 26, 30, 39, 45, 50, 54).

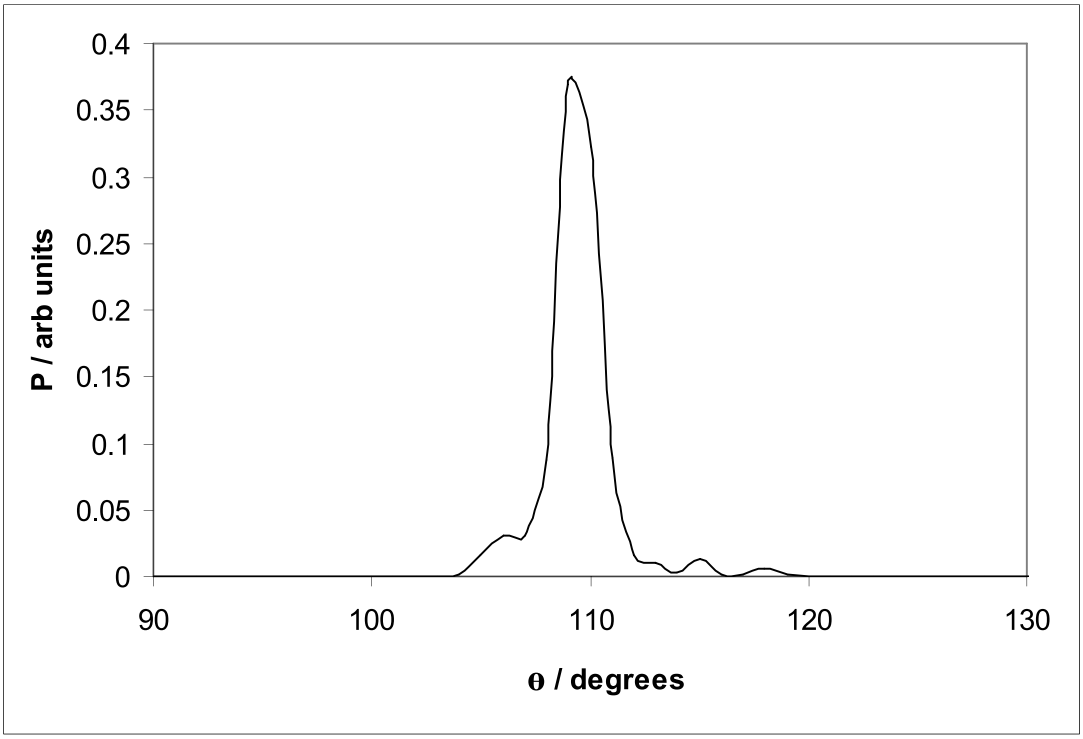
0.4
0.35
0.3
0.25
0.2
0.15
0.1
0.05
0
P / arb units
90
100
110
120
130
θ / degrees

V_6

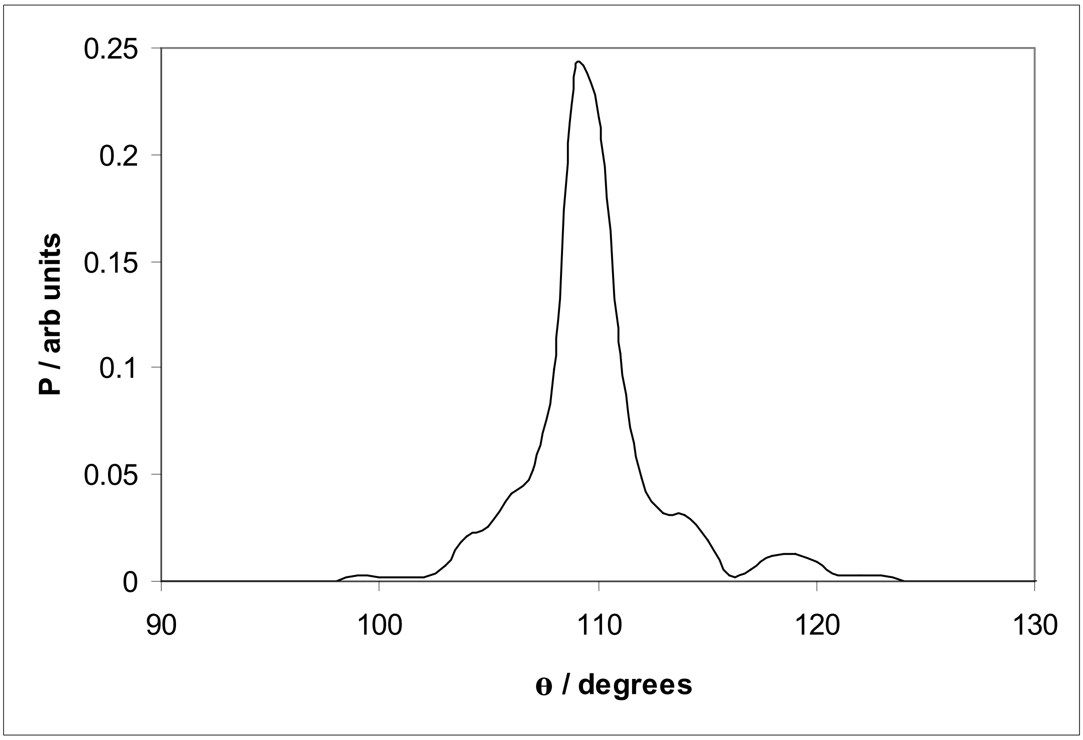
0.25
0.2
0.15
0.1
0.05
0
P / arb units
90
100
110
120
130
θ / degrees

V_{14}

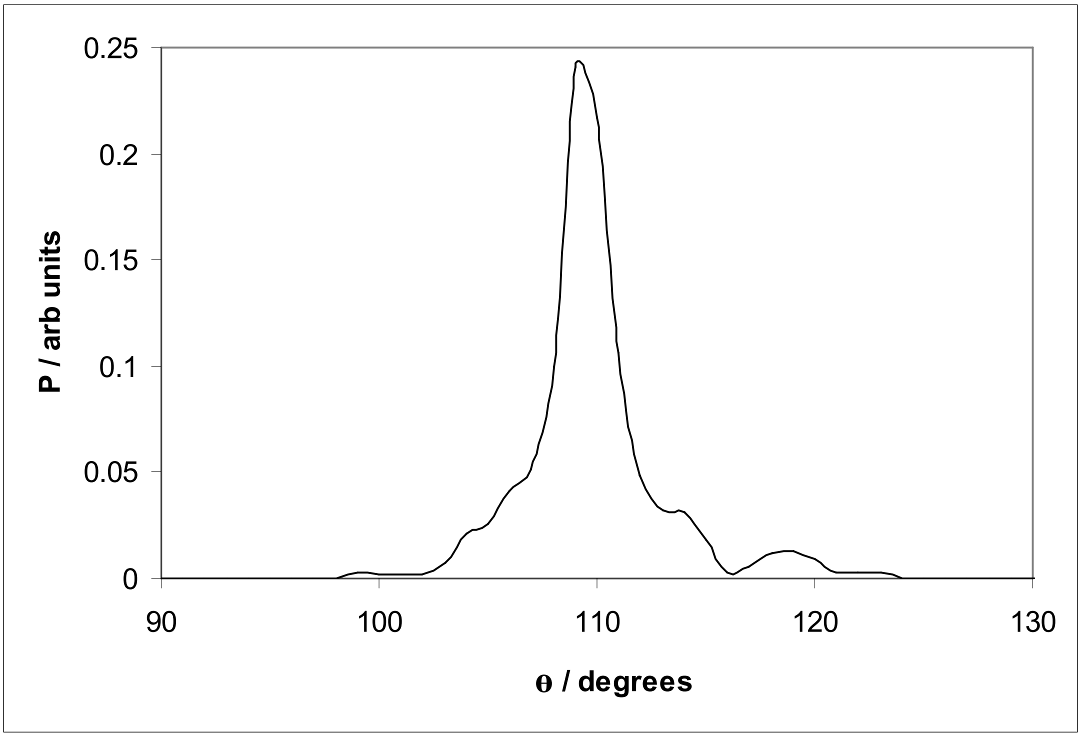
0.25
0.2
0.15
0.1
0.05
0
P / arb units
90
100
110
120
130
θ / degrees

V_{19}

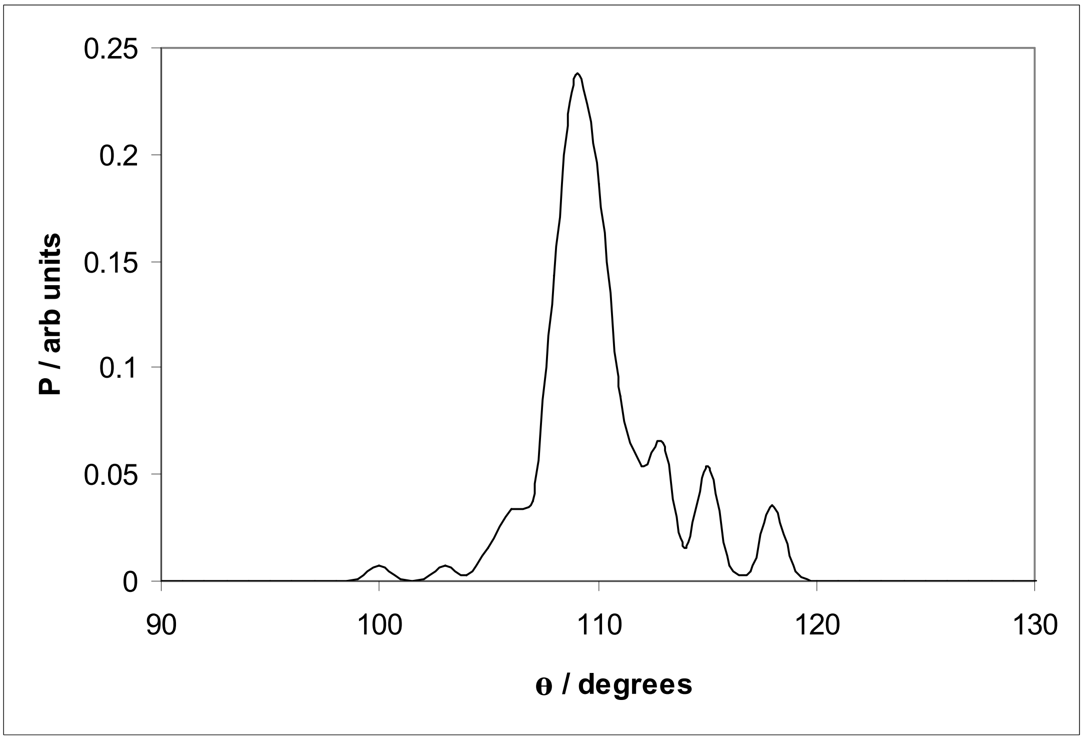
0.25
0.2
0.15
0.1
0.05
0
P / arb units
90
100
110
120
130
θ / degrees

V_{26}

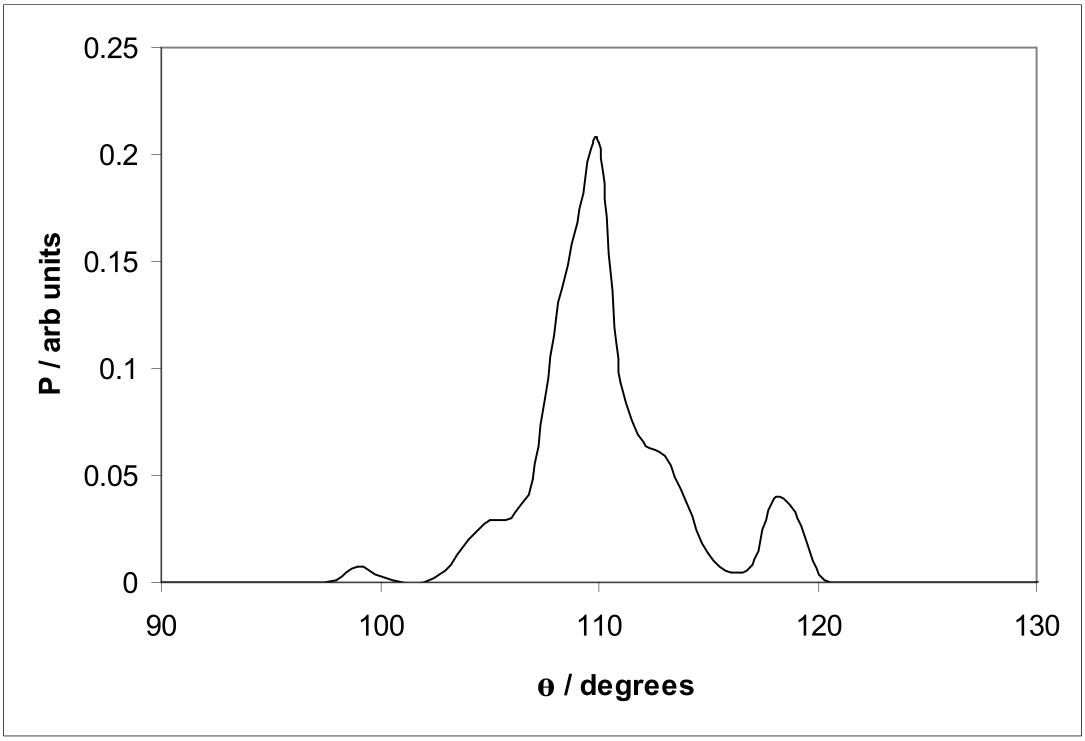
0.25
0.2
0.15
0.1
0.05
0
P / arb units
90
100
110
120
130
θ / degrees

V_{30}

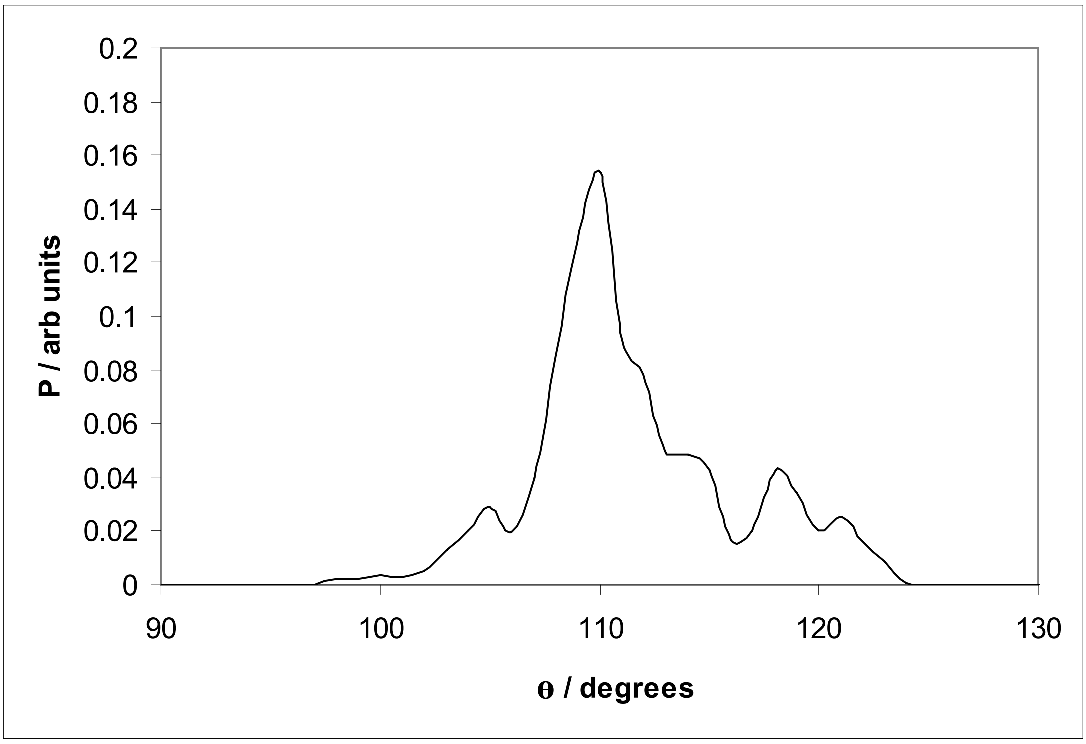
0.2
0.18
0.16
0.14
0.12
0.1
0.08
0.06
0.04
0.02
0
P / arb units
90
100
110
120
130
θ / degrees

V_{39}

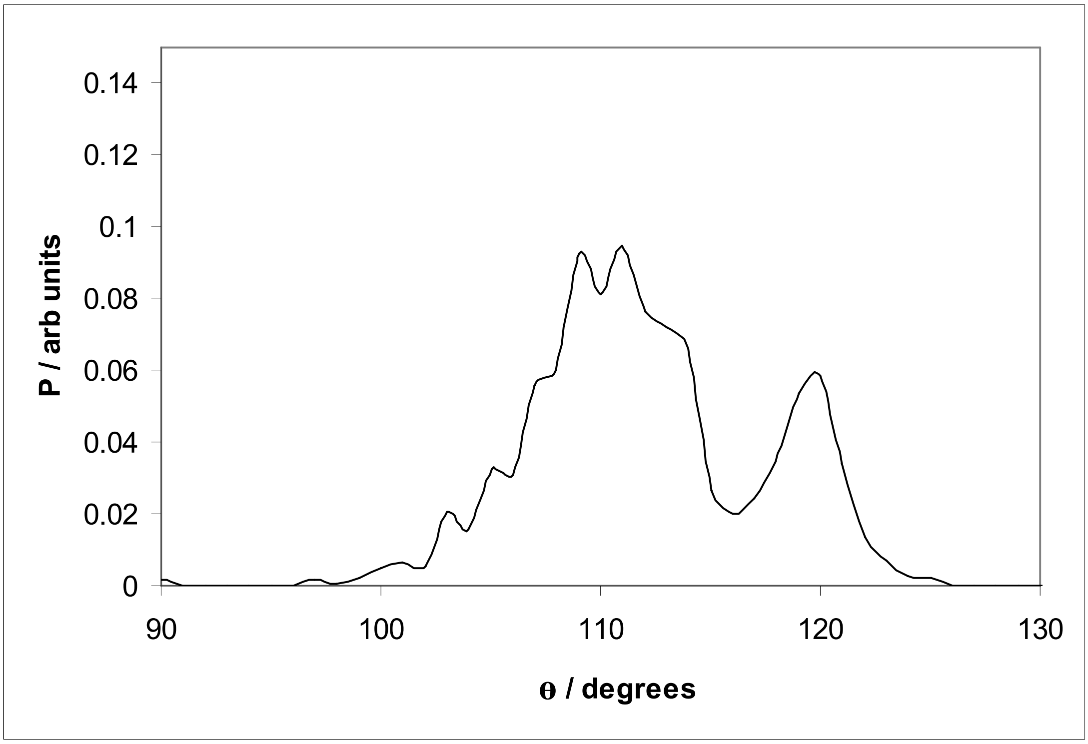
0.14
0.12
0.1
0.08
0.06
0.04
0.02
0
P / arb units
90
100
110
120
130
θ / degrees

V_{45}

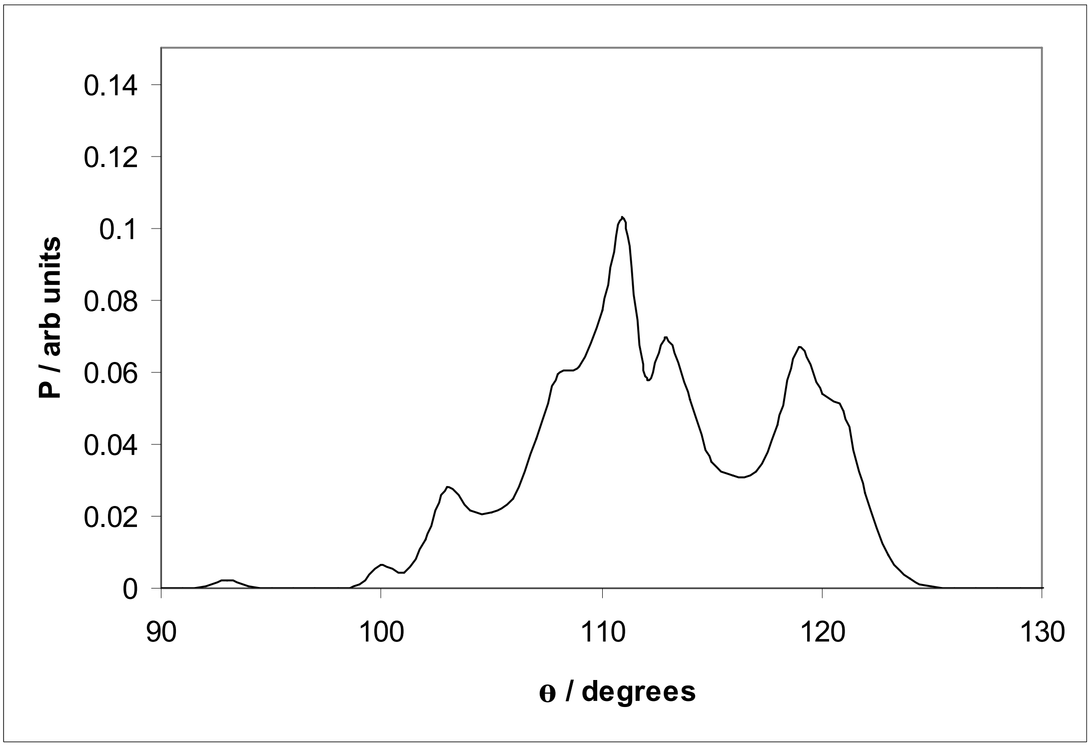
0.14
0.12
0.1
0.08
0.06
0.04
0.02
0
P / arb units
90
100
110
120
130
θ / degrees

V_{50}

This journal is © the Owner Societies 2010

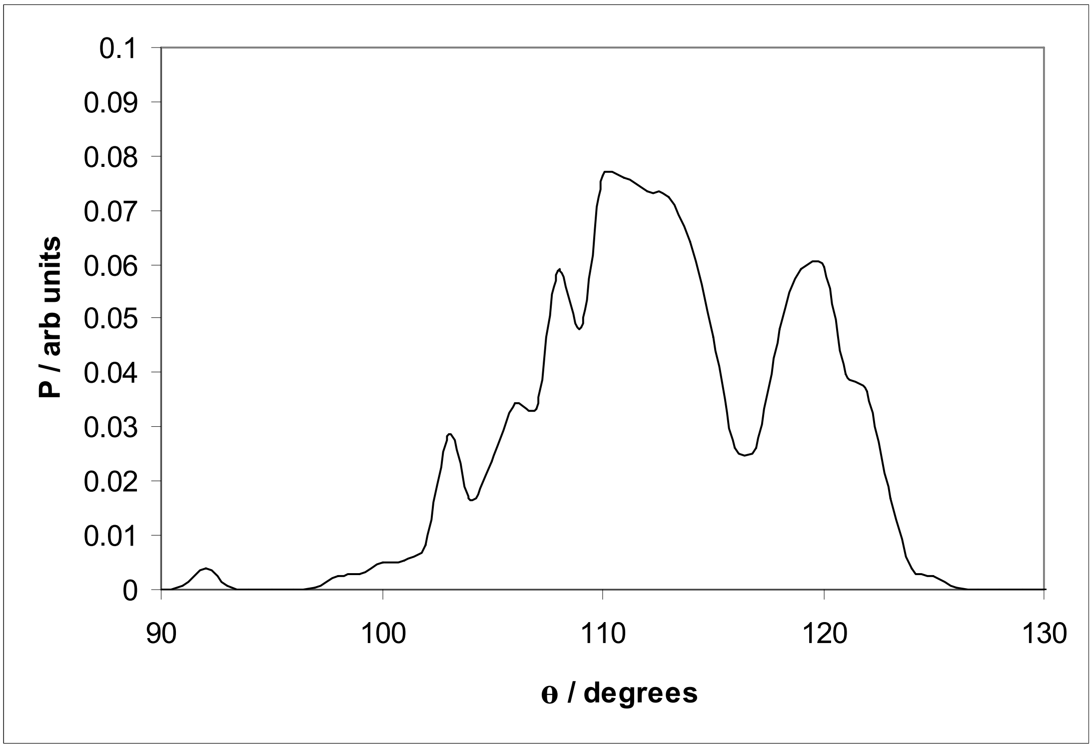

V_{54}

Figure S4. Calculated bond angle distribution function, P, for V_n in the $90 < \Theta < 130$ range. No angles are observed outside the presented range. (n=6, 14, 19, 26, 30, 39, 45, 50, 54).